

gy $E_0(3)$ of neon and argon inert-gas trimers (Lennard-Jones 12-6 pair potentials) than resulted from a recent variational calculation.²

*Permanent address: Department of Physics, University of Wisconsin, Madison, Wis. 53706. Work of this author supported in part by the National Science Foundation through the U. S.-Japan cooperative Science Program and in part by the Wisconsin Alumni Research Foundation.

¹We assume the integrals $\int_0^\infty dr r^2 \varphi^2(r)$ and $\int_0^\infty dr r \varphi^2$ are finite. The case of a zero-range force must be treated as a limiting case.

²L. W. Bruch and H. Stenschke, *J. Chem. Phys.* **57**, 1019 (1972).

Role of Angular Momentum in Complete Fusion Reactions:



A. M. Zebelman

York College of the City University of New York, Jamaica, New York 11432, and Department of Chemistry, Columbia University, New York, New York 10027

and

J. M. Miller

Department of Chemistry, Columbia University, New York, New York 10027

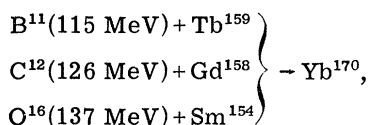
(Received 24 October 1972)

Measurements are reported for the complete-fusion cross sections in the reactions of $B^{11} + Tb^{159}$, $C^{12} + Gd^{158}$, and $O^{16} + Sm^{154}$ at bombarding energies such that the excitation energy of the Yb^{170} compound nuclei that are formed is 107 MeV. The results indicate that the complete-fusion cross sections are determined by dynamical processes in the entrance channel rather than by the equilibrium properties of the compound system.

There has recently been much interest in the experimental and theoretical determination of complete-fusion cross sections in heavy-ion-induced reactions, motivated primarily by the desire to investigate the feasibility of reactions designed to produce superheavy elements.¹⁻³

In a recent paper Blann and Plasil³ calculate complete-fusion cross sections, as they are operationally defined by current experimental techniques, through the use of an angular-momentum-dependent formalism which accounts for the non-compound portion of total reaction cross sections by considering it to be a type of fission. We report here complete-fusion cross sections which indicate that this point of view cannot be a complete picture of the phenomena that are involved.

Measurements have been made of the complete-fusion cross sections for the following entrance channels leading to the formation of the Yb^{170} compound nucleus with 107-MeV excitation energy:



where the laboratory energies of the incident heavy ions are given in parentheses for each entrance channel.

The data were collected at the Yale University heavy-ion accelerator. Isotopically enriched targets for the C^{12} and O^{16} entrance channels were obtained from Oak Ridge National Laboratory and are 1.0 mg/cm² and 0.87 mg/cm² thick, respectively. The target of Tb^{159} , an isotope which occurs with 100% natural abundance, was made by evaporating the metal onto a 40- $\mu\text{g}/\text{cm}^2$ carbon foil. The thickness was determined by elastic scattering to be 0.16 mg/cm².

Following the technique of Kowalski, Jodogne, and Miller¹ and Natowitz,² the complete-fusion cross sections were measured with mica detectors. The pieces of mica were etched prior to bombardment for 3 h in 48% hydrofluoric acid in order to enlarge any pre-existing tracks. Following bombardments, the tracks in the mica detectors were developed by again exposing the mica to 48% hydrofluoric acid for about 30 min. The detectors were then scanned under a microscope and a record was kept of the number of complete-fusion events corresponding to a known

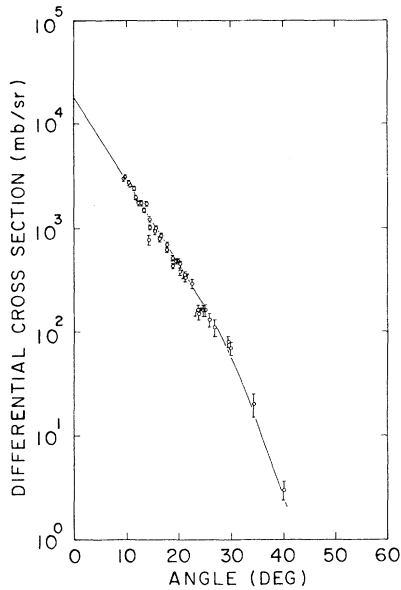


FIG. 1. Laboratory angular distribution of heavy recoils from $B^{11} + Tb^{159}$ ($E_{\text{bomb}} = 115$ MeV).

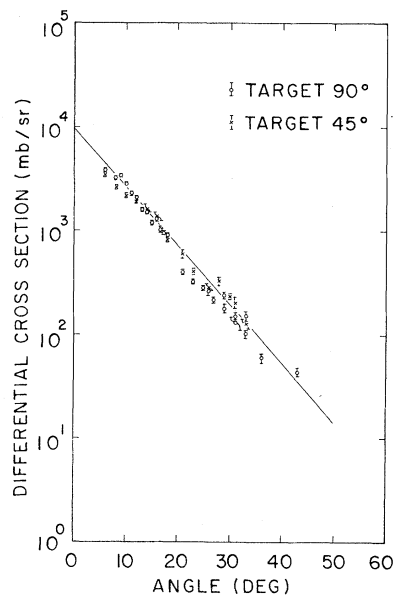


FIG. 2. Laboratory angular distribution of heavy recoils from C^{12} and Gd^{158} ($E_{\text{bomb}} = 126$ MeV).

laboratory angle and solid angle. More complete experimental details will follow in subsequent publications.

Suffice it to say here that there are two possible sources of uncertainty in the use of track detectors in this type of experiment which must be guarded against.

(1) Less than unit efficiency in the registration of heavy recoils. This would result from the kinetic energy of the recoils being below that for registration with unit probability. That this is not a problem in the present experiment is shown by the fact that the experimental results are the same when the target is changed from 45° to 90° with respect to the beam, thereby changing the amount of energy lost by the recoils in traversing the target.

(2) Registration of noncomplete-fusion events. This could result from either the transfer of at least approximately six charges from the target to the projectile with a concomitant small momentum transfer or, conversely, from a nearly complete momentum transfer from projectile to target with or without the transfer of nucleons. Both of these processes, like all energetically allowed events, doubtless have a nonzero cross sections; but from all that is known about the systematics of scattering and transfer reactions, the cross sections are probably immeasurably small with the techniques used here and are certainly within the quoted errors.

The complete-fusion angular distributions for the B^{11} , C^{12} , and O^{16} entrance channels are given in Figs. 1, 2, and 3. The total cross sections for the production of compound-nucleus recoils, calculated by integrating these distributions, are given in Table I. Table I also lists the fission cross sections for these entrance channels. The fission data for the C^{12} and O^{16} entrance channels have previously been published.⁴ The fission cross

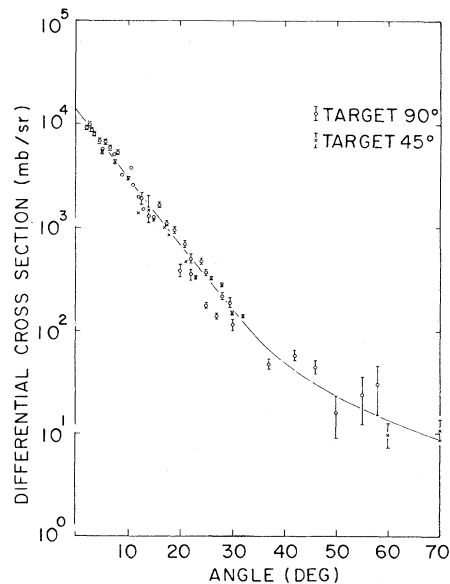


FIG. 3. Laboratory angular distribution for heavy recoils from $O^{16} + Sm^{154}$ ($E_{\text{bomb}} = 137$ MeV).

TABLE I. Cross sections in corresponding entrance channels.

Entrance channel	Heavy-recoil cross section (mb)	Fission cross section (mb)	Complete-fusion cross section (mb)
B ¹¹	973 ± 146	5.9 ± 0.6	979 ± 146
C ¹²	1080 ± 162	16 ± 1.6	1096 ± 162
O ¹⁶	1222 ± 183	40 ± 4.0	1262 ± 183

section for the B¹¹ entrance channel was measured in the same fashion as that previously described.⁴ The last column in Table I gives the total complete-fusion cross sections which are the sums of the total compound-nucleus-recoil cross sections and the total fission cross sections in each entrance channel. The symmetric nature of the fission-fragment angular distributions⁴ and the results of Sikkeland and Viola⁵ support the notion that the fission process for the system studied here is compound nuclear in nature; therefore, the fission cross section is included in the complete-fusion cross sections. It is to be noted, though, that the calculation of Blann and Plasil³ would specifically not include the fission cross section as part of the complete-fusion cross section. This is perhaps a moot point for the systems of present concern since the fission cross sections are all quite small compared to the compound-nuclear-recoil cross sections.

Having briefly presented the experimental data, we turn now to a comparison of those data to the formalism of Blann and Plasil.

The complete-fusion cross section, $\sigma_{cf}(x)$, for a given entrance channel x may be expressed as

$$\sigma_{cf}(x) = \pi \lambda_x^2 \sum_{l=0}^{\infty} (2l+1) T_{l, cf}, \quad (1)$$

where λ_x is the reduced wavelength in entrance channel x , l is the orbital angular momentum, and $T_{l, cf}$ is the transmission coefficient for orbital angular momentum l corresponding to the complete fusion of the target and incident projectile. In the Blann-Plasil calculation the quantities $T_{l, cf}$ are effectively given by $T_l P_{l, cf}$, where T_l is the usual transmission coefficient for partial wave l calculated via the optical model and $P_{l, cf}$ is the probability that the compound nucleus formed from the l th partial wave survives de-excitation without fissioning. Thus, Eq. (1) takes the form

$$\sigma_{cf}(x) = \pi \lambda_x^2 \sum_{l=0}^{\infty} (2l+1) T_l(x) P_{l, cf}. \quad (2)$$

It is to be noted that the quantity $P_{l, cf}$ depends only on the compound nucleus that is formed and thus should be the same for the three entrance channels discussed in this paper. Further, if the $T_l(x)$ were all unity over the range of l , where $P_{l, cf}$ is nonzero for all three entrance channels, then the term in the summation would be independent of entrance channel and, hence, the quantities $\sigma_{cf}(x)/\lambda_x^2$ would also be independent of entrance channel. Column 3 of Table II shows that this quantity is not independent of entrance channel.

It remains to examine the assumption that the $T_l(x)$ are all unity over the range where $P_{l, cf}$ is nonzero. To that end, it is useful to compare the results of the well-known sharp-cutoff model for complete-fusion cross sections with the optical-model transmission coefficients. In this context the sharp cutoff model merely means that the quantity $P_{l, cf}$ is unity below some critical value of l , l_{crit} , and vanishes for higher values of l . The quantity l_{crit} is calculated by requiring that

$$\sigma_{cf}(x) = \pi \lambda_x^2 \sum_{l=0}^{l_{crit}} (2l+1) T_l. \quad (3)$$

The results of such a comparison are shown in Fig. 4 where the T_l were obtained from the ABA-CUS-2 code⁶ using the optical-model parameters given by Auerbach and Porter.⁷ From that figure it is clear that the T_l are indeed unity in all of the entrance channels over the region where $P_{l, cf}$ is nonzero. If the sharp-cutoff requirement is

TABLE II. Reduced heavy-recoil cross sections.

Entrance channel	λ^2 (mb)	$\frac{\sigma(\text{heavy recoil})}{\lambda^2} \times 10^{-4}$
B ¹¹	0.0188	5.2 ± 0.8
C ¹²	0.0159	6.8 ± 1.0
O ¹⁶	0.0116	10.5 ± 1.6

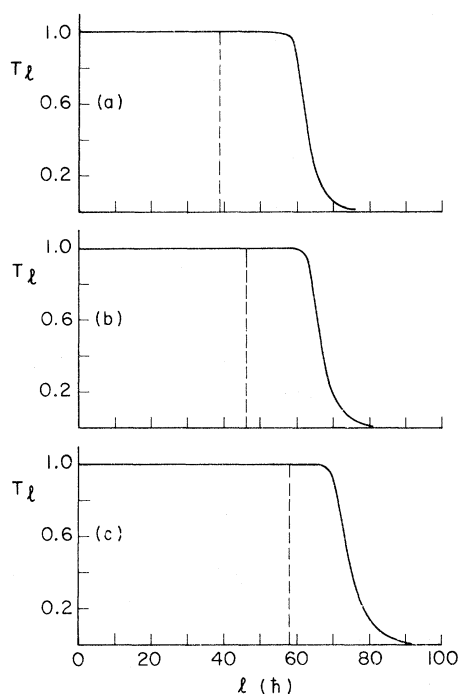


FIG. 4. (a) Transmission coefficients for $B^{11} + Tb^{159}$ with sharp-cutoff approximation to $l_{crit}(B^{11})$ indicated by dashed line. (b) Transmission coefficients for $C^{12} + Gd^{158}$ with sharp-cutoff approximation to $l_{crit}(C^{12})$ indicated by dashed line. (c) Transmission coefficients for $O^{16} + Sm^{154}$ with sharp-cutoff approximation to $l_{crit}(O^{16})$ indicated by dashed line.

relaxed in a fashion described by Blann and Plasil (cf. Fig. 2 of Ref. 3) there is but a small change in the range of l over which $P_{l, cf}$ is non-zero. Thus, we conclude that the divergences in the values of $\sigma_{cf}(x)/\lambda_x^2$ are not a consequence of the T_l values differing from unity, but rather that the model underlying Eq. (2) is not a complete description of the phenomena that are in-

involved. Indeed, just the fact that the sharp-cutoff values of l_{crit} are different for each of the entrance channels, as may be seen in Fig. 4, leads immediately to the same conclusion. Evidently, the processes that compete with complete fusion are not determined only by the equilibrium properties of the compound nuclei that are formed. Rather, they seem to entail the dynamics of the entrance channel in an essential manner. While it is doubtless true that there is some critical range of l determined by equilibrium properties above which the complete-fusion product cannot stick together, at least in the systems studied here there seems to be a lower-valued critical range of l determined by the dynamical properties of each entrance channel that govern the complete-fusion cross sections.

†Work supported in part by the U. S. Atomic Energy Commission.

¹L. Kowalski, J. C. Jodogne, and J. M. Miller, *Phys. Rev.* **169**, 894 (1968).

²J. B. Natowitz, *Phys. Rev. C* **1**, 623 (1970).

³M. Blann and F. Plasil, *Phys. Rev. Lett.* **29**, 303 (1972).

⁴L. Kowalski, A. Zebelman, A. Kandil, and J. M. Miller, *Phys. Rev.* **3**, 1370 (1971).

⁵T. Sikkeland and V. F. Viola, Jr., in *Proceedings of the Third Conference on Reactions Between Complex Nuclei*, edited by A. Ghiorso, R. M. Diamond, and H. E. Conzett (Univ. of California Press, Berkeley, 1963), p. 232.

⁶ABACUS-2, E. H. Auerbach, BNL Report No. 4562, 1962 (unpublished).

⁷E. H. Auerbach and C. E. Porter, in *Proceedings of the Third Conference on Reactions Between Complex Nuclei*, edited by A. Ghiorso, R. M. Diamond, and H. E. Conzett (Univ. of California Press, Berkeley, 1963), p. 19.